

October 20, 2003

## Spontaneous magnetization and electron momentum density in three-dimensional quantum dots

R. Saniz

*Universidad Catolica Boliviana*

B. Barbiellini

*Northeastern University*

A. B. Denison

*Lawrence Livermore National Laboratory*

A. Bansil

*Northeastern University*

---

### Recommended Citation

Saniz, R.; Barbiellini, B.; Denison, A. B.; and Bansil, A., "Spontaneous magnetization and electron momentum density in three-dimensional quantum dots" (2003). *Physics Faculty Publications*. Paper 431.

**Spontaneous magnetization and electron momentum density in three-dimensional quantum dots**

 R. Saniz,<sup>1</sup> B. Barbiellini,<sup>2</sup> A. B. Denison,<sup>3</sup> and A. Bansil<sup>2</sup>
<sup>1</sup>*Departamento de Ciencias Exactas, Universidad Católica Boliviana, Casilla #5381, Cochabamba, Bolivia*
<sup>2</sup>*Physics Department, Northeastern University, Boston, Massachusetts 02115, USA*
<sup>3</sup>*Lawrence Livermore National Laboratory, 7000 East Avenue, Livermore, California 94550-9234, USA*

(Received 6 August 2003; published 20 October 2003)

We discuss an exactly solvable model Hamiltonian for describing the interacting electron gas in a quantum dot. Results for a spherical square-well confining potential are presented. The ground state is found to exhibit striking oscillations in spin polarization with dot radius at a fixed electron density. These oscillations are shown to induce characteristic signatures in the momentum density of the electron gas, providing a route for direct experimental observation of the dot magnetization via spectroscopies sensitive to the electron momentum density.

DOI: 10.1103/PhysRevB.68.165326

PACS number(s): 73.22.Dj, 75.10.-b, 75.75.+a

Quantum dots (QDs), which may be thought of as artificial “atoms,” not only provide a nanoscale laboratory for fundamental quantum mechanical studies, but also hold the promise of spintronic and other applications.<sup>1–4</sup> Spin polarization in nanosystems is therefore drawing great attention in view of its intrinsic importance,<sup>5–7</sup> and its possible relationship to other phenomena, such as kinks in the positions of Coulomb blockade peaks in two-dimensional (2D) QDs,<sup>8</sup> or the so-called 0.7 conduction anomaly in quantum point contacts.<sup>9</sup> In 2D dots, experiments point to shell-like filling of levels in accord with Hund’s first rule,<sup>5</sup> and a recent spin density-functional calculation indicates the presence of a ground state with high spin in relatively large dots.<sup>10</sup> In 3D dots, shell structure of energy levels has been reported,<sup>11</sup> and results on the fine structure in the energy spectra of gold nanoparticles have been interpreted in terms of a ground state spin magnetization larger than 1/2.<sup>12</sup> However, Ref. 13 argues that in finite disordered systems fluctuations in off-diagonal interaction matrix elements may suppress ground state magnetization. It is clear that the spin polarization of QDs is a subject of considerable current interest and controversy.

In this work, we develop an exactly solvable many-body model Hamiltonian of wide applicability for describing correlated electrons confined to a QD. The ground state is clearly found to exhibit spontaneous magnetization and strong oscillations in spin polarization as a function of the dot radius. In order to identify observable signatures of the remarkable aforementioned oscillations in polarization, we consider the dot electron momentum density (EMD) at some length. The key quantity in this connection turns out to be the width  $\Delta p$  over which the EMD falls to zero around the Fermi cutoff momentum. In particular, oscillations in magnetization are shown to induce similar oscillations in  $\Delta p$ , indicating that this effect would be amenable to direct experimental observation via EMD spectroscopies, such as angular correlation of positron annihilation radiation (ACAR) and Compton scattering. Our results also bear more broadly on the applications of QDs in that they point to the possibility of having a system in a ferromagnetic ground state with no low temperatures and/or external magnetic fields.

We consider the Hamiltonian

$$\hat{H} = \sum_{\nu\sigma} \epsilon_{\nu}^0 a_{\nu\sigma}^{\dagger} a_{\nu\sigma} + \frac{1}{2} U \sum_{\nu\nu'\sigma} a_{\nu\sigma}^{\dagger} a_{\nu'-\sigma}^{\dagger} a_{\nu'-\sigma} a_{\nu\sigma}. \quad (1)$$

The first term ( $\hat{H}_0$ ) describes the noninteracting system. It corresponds to the spherical square well:  $V(r) = -V_0$ , for  $r \leq R$ , and  $V(r) = 0$  otherwise, and the associated one-particle eigenfunctions  $\varphi_{\nu}$  with eigenvalues  $\epsilon_{\nu}^0$ ;  $\nu \equiv nlm$  is a composite index and  $\sigma$  labels spin. The second term ( $\hat{H}_I$ ) describes the interaction and allows Coulomb repulsion via the parameter  $U$  only between electrons of opposite spin—electrons of like spin being kept apart by the Pauli exclusion principle. In this connection, we have carried out extensive numerical estimates, and find that direct Coulomb matrix elements are larger, on an average, by an order of magnitude or more, than exchange or other terms for dot radii up to 30 Å and electron densities ranging from  $r_s = 2$  to 5 (Bohr radii).<sup>14</sup> Spin-orbit effects here are also expected to be small, since the confining potential is relatively weak due to the screening of the nuclei by the core electrons. For these reasons, form (1) should provide a reasonable model for the electronic structure of 3D QDs.

The standard one-particle Green function for the many electron system can be expanded as

$$\mathcal{G}_{\sigma\sigma'}(\mathbf{r}\mathbf{r}', \tau) = \sum_{\nu\nu'} \varphi_{\nu}^*(\mathbf{r}) \varphi_{\nu'}(\mathbf{r}') \mathcal{G}_{\sigma\sigma'}(\nu\nu', \tau),$$

with  $\mathcal{G}_{\sigma\sigma'}(\nu\nu', \tau) = -\langle T_{\tau} a_{\nu\sigma}(\tau) a_{\nu'\sigma'}^{\dagger}(0) \rangle$ . It is readily shown that

$$\hbar \partial a_{\nu} / \partial \tau = -\xi_{\nu} a_{\nu\sigma} - U \hat{N}_{-\sigma} a_{\nu\sigma},$$

where  $\xi_{\nu} = \epsilon_{\nu}^0 - \mu$  ( $\mu$  is the chemical potential), and  $\hat{N}_{-\sigma} = \sum_{\nu'} a_{\nu'-\sigma}^{\dagger} a_{\nu'-\sigma}$ . Then, the equation of motion for  $\mathcal{G}_{\sigma\sigma'}(\nu\nu', \tau)$  is

$$\begin{aligned} -\hbar \frac{\partial}{\partial \tau} \mathcal{G}_{\sigma\sigma'}(\nu\nu', \tau) &= \hbar \delta_{\sigma\sigma'} \delta_{\nu\nu'} \delta(\tau) + \xi_{\nu} \mathcal{G}_{\sigma\sigma'}(\nu\nu', \tau) \\ &\quad - U \langle T_{\tau} \hat{N}_{-\sigma}(\tau) a_{\nu\sigma}^{\dagger}(\tau) a_{\nu'\sigma'}^{\dagger}(0) \rangle. \end{aligned} \quad (2)$$

Since our Hamiltonian possesses the property that  $[\hat{H}_l, \hat{H}_0 - \mu\hat{N}] = 0$ , Wick's theorem allows us to factorize the preceding ground state average, i.e.,

$$\langle T_\tau \hat{N}_{-\sigma}(\tau) a_{\nu\sigma}^\dagger(\tau) a_{\nu'\sigma'}^\dagger(0) \rangle = -N_{-\sigma} \mathcal{G}_{\sigma\sigma'}(\nu\nu', \tau),$$

where  $N_{-\sigma} = \sum_{\nu'} f_{\nu'-\sigma}$ , with  $f_{\nu'-\sigma}$  denoting the Fermi occupation function. A Fourier transform in  $\tau$  immediately yields the *exact* Green function

$$\mathcal{G}_{\sigma\sigma'}(\nu\nu', i\omega_n) = \delta_{\sigma\sigma'} \delta_{\nu\nu'} \frac{1}{i\omega_n - \xi_\nu/\hbar - U N_{-\sigma}/\hbar}. \quad (3)$$

The self-energy thus is  $\Sigma_\sigma^* = U N_{-\sigma}/\hbar$ . The interacting energy levels  $\epsilon_{\nu\sigma}$  are given by the solutions of  $\omega - \xi_\nu/\hbar - \Sigma_\sigma^* = 0$  (frequencies measured with respect to  $\mu/\hbar$ ) minimizing the ground state energy,  $E = \sum_{\nu\sigma} (\epsilon_\nu^0 + \frac{1}{2} \hbar \Sigma_\sigma^*) f_{\nu\sigma}$ . Given the number of particles  $N$ , this defines a set of nonlinear equations for the populations,  $N_\uparrow$  and  $N_\downarrow$ , of up and down spin states, respectively. The resulting splitting in energy for states of opposite spin,  $\Delta = U(N_\uparrow - N_\downarrow)$ , is *uniform*, i.e., it does not depend on the quantum numbers  $\nu$ . Note that, although the total wave function corresponding to our solution has the form of an unrestricted Hartree-Fock wave function, it does not suffer from the so-called spin contamination problem and is a spin eigenfunction. This is because the single-particle wave functions in our case are orthonormal, and we have  $\hat{S}^2 = \hat{S}_z(\hat{S}_z + 1)$ .<sup>15</sup> Also note that temperature enters our formulas only through the Fermi function  $f_{\nu\sigma}$ ; all results in the remainder of this article refer to the zero temperature limit.

We comment briefly on the nature of the four essential parameters which describe our model:  $r_s$ , the electron density;  $R$ , the dot radius or, equivalently, the number  $N$  of electrons [ $N = (R/r_s)^3$ ];  $V_0$ , the well-depth; and,  $U$ , the Coulomb energy. The values of  $r_s$  and  $R$  are related to the type and size of the systems considered. In this study we use  $r_s = 5$ , a relatively low density, enabling us to consider a wide range of dot radii.  $V_0$  may then be obtained reasonably in terms of the work function of the system studied and the Fermi energy of the free electron gas with the same  $r_s$ . For  $r_s = 5$ , following Ref. 16, we take  $V_0 = 8.62$  eV. The choice of the remaining parameter  $U$  is somewhat tricky, mainly because correlations in QDs are not well understood. A handle on  $U$  can be obtained by considering the average value  $U_{TF}$  of the Thomas-Fermi (TF) screened Coulomb interaction,  $\int d\mathbf{r} d\mathbf{r}' |\varphi_\nu(\mathbf{r})|^2 v_{TF}(|\mathbf{r} - \mathbf{r}'|) |\varphi_\mu(\mathbf{r}')|^2$ , averaged over all occupied states in the *noninteracting* system, with  $v_{TF}(r) = e^2 \exp(-r/l_{TF})/r$ , where  $l_{TF} = \sqrt{r_s}/1.56$  is the TF screening length. However, actual screening in real materials is likely to be weaker. For example, in noble metals, an effective screening length  $l_{TF}/0.73$  is reported.<sup>17</sup> Using this value, we find an enhanced Coulomb interaction given roughly by  $1.75U_{TF}$ , which is the value we have used throughout this work.

Figure 1 illustrates the nature of the energy levels  $\epsilon_{\nu\sigma}$  for a 12.11 Å radius dot, for which  $N = 96$  and  $U = 27.13$  meV ( $U_{TF} = 15.50$  meV). The self-consistent splitting between up

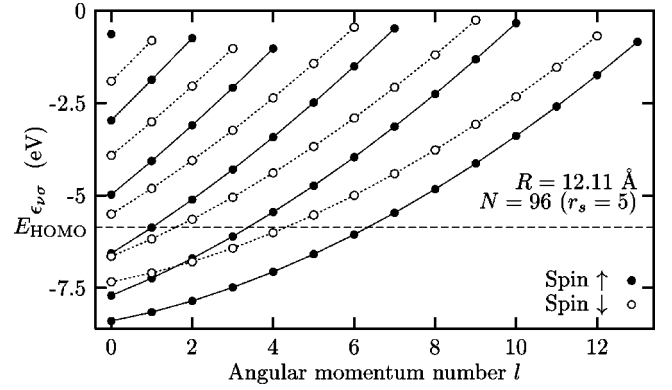


FIG. 1. Typical energy spectrum  $\epsilon_{\nu\sigma}$  for the interacting Hamiltonian (1). Filled (open) circles give majority (minority) spin levels, those with equal  $n$  joined by solid (dotted) lines for clarity. Levels possess a degeneracy of  $2l+1$ . Horizontal dashed line marks the highest occupied molecular-orbital energy,  $E_{HOMO}$ .

and down spin electrons is found to be  $\Delta = 1.03$  eV. The highest occupied molecular-orbital (HOMO) energy level is  $E_{HOMO} = -5.86$  eV, which may be thought of as the dot “Fermi energy.” We have  $N_\uparrow = 67$  and  $N_\downarrow = 29$ , so that the ground state spin polarization per electron is  $\zeta = (N_\uparrow - N_\downarrow)/N = 0.4$ .

We discuss now  $\zeta$  as a function of dot radius with reference to Fig. 2. In the weakly interacting limit ( $U \rightarrow 0$ ),  $\Delta \rightarrow 0$ , still the degeneracy between up and down spin in the  $nl$  shells is lifted, and as Fig. 2(a) clearly shows, shells fill in accord with Hund's first rule. Indeed, as the number of particles increases with dot radius, the spin polarization reaches a peak each time a shell is half filled with up-spin electrons, and falls to zero when the shell is completed with down-spin electrons. The sequence of these so-called “magic numbers,” i.e.,  $N$  values for which all occupied shells are completely filled, will of course differ here from that in atoms or 2D QDs due to differences in the details of the underlying spec-

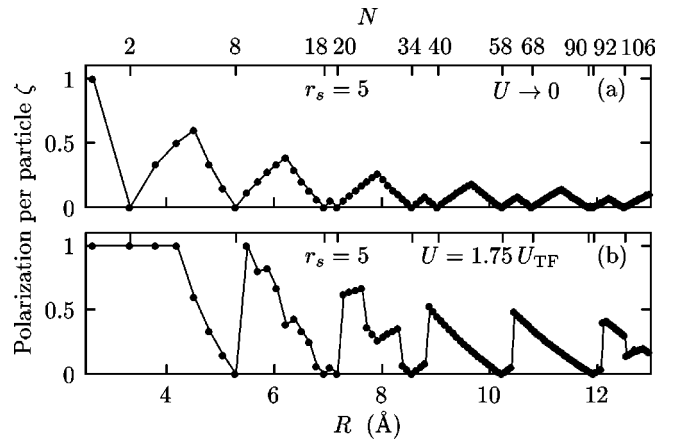


FIG. 2. Spin polarization per particle,  $\zeta = (N_\uparrow - N_\downarrow)/N$ , as a function of the dot radius  $R$ . Computed values (filled circles) are connected by solid lines to guide the eye. Number of electrons  $N$  is indicated on the top axis. (a) Weakly interacting case,  $U \rightarrow 0$ . (b) Strongly interacting case,  $U = 1.75U_{TF}$ .

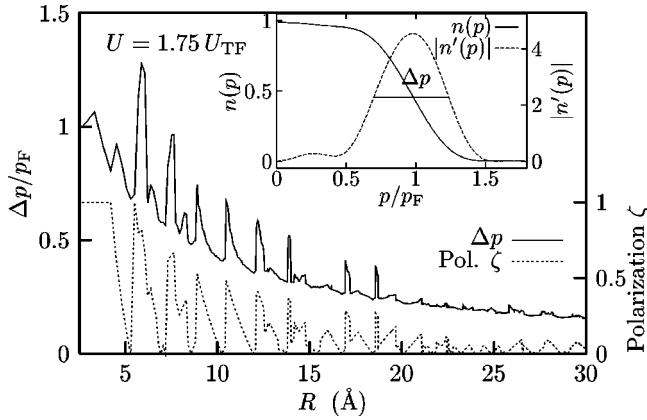


FIG. 3. *Inset:* Typical electron momentum density,  $n(p)$ , and the magnitude of its first derivative,  $|n'(p)|$ ; curves are normalized by  $V/4\pi^3$ , where  $V$  is the dot volume. The position of the peak in  $|n'(p)|$  defines the dot “Fermi momentum,” while its full-width-at-half-maximum (FWHM) defines  $\Delta p$ . *Main graph:*  $\Delta p$  in reduced units of  $p_F$  (solid line, left scale), and spin polarization  $\zeta$  (dotted, right scale) vs dot radius  $R$ .

trum. The magic numbers up to 106 are indicated on the upper axis in Fig. 2(a). Turning next to the strongly interacting case, Fig. 2(b) shows large deviations in  $\zeta$  from a simple Hund’s rule filling.<sup>18</sup> This is because  $\Delta$  changes with each added electron in order to minimize the total energy. The first four electrons enter the up-spin  $1s$  and  $1p$  levels, so that  $\zeta = 1$ , while the next four enter the corresponding down spin levels until  $\zeta$  vanishes for  $N=8$ . The ninth electron induces a strong change in  $\Delta$ , so that the  $1s$  and  $1p$  down-spin levels are pushed above the  $1d$  up-spin level, causing the former to empty in favor of the latter and the system to become completely polarized again. Similar level reorderings are involved in the other “kinks” seen in Fig. 2(b).

In order to identify observable signatures of the remarkable changes in the polarization depicted in Fig. 2, we consider the EMD, defined by

$$n(\mathbf{p}) = (2\pi)^{-1} \int_{-\infty}^{\infty} d\omega f(\omega) A(\mathbf{p}, \omega),$$

where  $f$  is the Fermi function and  $A$  is the spectral function  $A(\mathbf{p}, \omega) = -2 \text{Im} G^R(\mathbf{p}, \omega)$ , with  $G^R(\mathbf{p}, \omega) = \mathcal{G}(\mathbf{p}, i\omega_n \rightarrow \omega + i\delta)$ . The inset in Fig. 3 illustrates  $n(p)$  and the magnitude of its first derivative  $|n'(p)|$  for the same parameter values as in Fig. 1. The region of rapid variation in  $n(p)$  can be characterized via the position  $p_F$  of the peak in  $|n'(p)|$  and the associated full-width-at-half-maximum (FWHM),  $\Delta p$ . In the bulk limit in a metallic system  $p_F$  will tend to the Fermi momentum, where  $n(p)$  will develop a break and  $|n'(p)|$  a  $\delta$ -function peak, correspondingly. For simplicity, therefore, we may refer to  $p_F$  loosely as the dot “Fermi momentum,” even though there are no breaks in the EMD in a finite system.<sup>19,20</sup> Figure 3 considers  $\Delta p$  systematically and shows the presence of a dramatic series of peaks (solid line) spaced more or less regularly as a function of  $R$ . A comparison with corresponding changes in  $\zeta$  (dotted curve), makes it evident that peaks in  $\Delta p$  are well correlated with those in  $\zeta$ , some

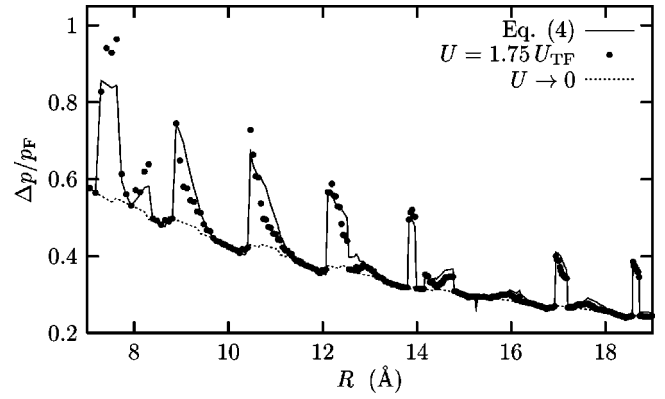


FIG. 4.  $\Delta p/p_F$  vs dot radius  $R$ , obtained from the approximate expression of Eq. (4) (solid line), compared with the exact result (bullets). The baseline corresponding to the noninteracting limit,  $\Delta p_0/p_F$ , is given (dotted) for reference.

differences notwithstanding. This correlation arises because, at a peak in  $\zeta$ , the up- and down-spin EMDs become substantially shifted with respect to each other, reflecting the polarization of the system, so that the EMD presents a much larger value of  $\Delta p$  overall. In short, peaks in  $\Delta p$  clearly are a signature of peaks in  $\zeta$ .<sup>21</sup>

Motivated by the preceding considerations, we have obtained an approximate expression for  $\Delta p$  as

$$\Delta p/p_F = \Delta p_0/p_F + c \Delta(\zeta - \zeta_0)R, \quad (4)$$

where  $\zeta_0$  is the spin polarization in the weakly interacting case ( $U \rightarrow 0$ ), and  $c$  is a constant, which depends on various dot parameters, with a fitted value in the present case of  $c = 4.29 \times 10^{-2} \text{ eV}^{-1} \text{ \AA}^{-1}$ . The first term in Eq. (4) describes the  $U \rightarrow 0$  limit and can be shown to follow the scaling law  $0.93 \text{ \AA}(r_s/a_0)/R$ .<sup>16</sup> The second term incorporates the effect of the spin polarization induced through the interaction  $U$ . Figure 4 shows that Eq. (4) provides an excellent description of the exact  $\Delta p$  data as a function of  $R$ . The approximation continues to be equally good up to  $R=30 \text{ \AA}$ , although for clarity results over a shorter  $R$  range are shown in the figure.

We emphasize that the form of our solution in Eq. (3) does not depend explicitly on that of the noninteracting Hamiltonian ( $\hat{H}_0$ ). Although details of  $\zeta$  will vary with those of the spectrum of  $\hat{H}_0$ , we expect our prediction of oscillations in  $\zeta$  with dot radius to be generally robust to changes in the shape and dimensionality of the confining potential.<sup>22,23</sup> Thus, we expect our results to be relevant to almost one-dimensional systems. Indeed, in metallic nanowires,<sup>24</sup> Zabala *et al.*<sup>6</sup> report a series of peaks in the magnetic moment per electron as a function of wire radius, correlated strongly with another observable of the system (the elongation force of the nanowire). The physics driving these results is similar to that in our work,<sup>25</sup> despite the fact that Ref. 6 considers the stabilized jellium model within the framework of the spin-dependent density-functional formalism, while we treat correlation effects differently, in terms of the direct interaction  $U$  and neglect various off-diagonal exchange and other contributions.<sup>26</sup>

The relationship between  $\zeta$  and  $\Delta p$  provides a powerful handle for a direct experimental verification of the polarization oscillations in QDs predicted in this study via the use of solid-state spectroscopies sensitive to the EMD, namely, angular correlation of positron-annihilation radiation (ACAR) [positrons have the advantage of being local probes, see Weber *et al.* in Ref. 19], inelastic x-ray scattering (IXS) in the deeply inelastic (Compton) regime and scanning tunneling microscopy (STM). We have carried out further computations at other  $r_s$  values and find that, generally speaking, polarization effects become less prominent with decreasing  $r_s$ , as the kinetic energy dominates, as well as with increasing  $R$ , as electrons are less confined and  $U$  becomes weaker. Nevertheless, oscillations in  $\Delta p$  are observable even for  $r_s \approx 3$ , particularly for dot sizes  $R \lesssim 10 \text{ \AA}$ .

In summary, we have presented an *exactly solvable* model Hamiltonian for discussing the properties of the interacting electron gas in the confined geometry of a QD. Although the results presented in this article are based on a confining potential in the shape of a spherical square-well, computations for other geometries and confining potentials would be quite straightforward. The ground state is found to exhibit spontaneous magnetization and striking oscillations in spin polar-

ization  $\zeta$  as a function of the dot radius  $R$ , at the fixed electron density considered. The oscillations in  $\zeta$  are shown to induce similar oscillations in the width  $\Delta p$  around the Fermi cutoff in the EMD, which we refer to for simplicity as the dot “Fermi momentum,” providing a route for direct experimental observation of the dot magnetization via spectroscopies sensitive to the EMD (specially, positron annihilation and Compton scattering). A simple expression for  $\Delta p$  is discussed, which gives an excellent approximation to the exact numerical data as a function of radius. We expect the results of the present study to be robust to the details of the confining potential and to the approximations inherent in the treatment of correlations in our model Hamiltonian.

This work was supported by the U.S. Department of Energy contracts nos. DE-AC03-76SF00098 and W-7405-ENG-48 and the U.S. Department of Energy Office of Basic Energy Science, Division of Materials Science, and benefited from the allocation of supercomputer time at the NERSC and the Northeastern University Advanced Scientific Computation Center (ASCC). We thank K.-F. Berggren for very useful discussions. R.S. acknowledges the hospitality and support of Northeastern University’s Physics Department during a research visit.

- <sup>1</sup>R.C. Ashoori, *Nature (London)* **379**, 413 (1996); L.P. Kouwenhoven, C.M. Marcus, P.L. McEuen, S. Tarucha, R.M. Westervelt, and N.S. Wingreen, in *Mesoscopic Electron Transport*, Vol. 345 of *NATO Advanced Studies Institute, Series E: Applied Sciences*, edited by L.L. Sohn, L.P. Kouwenhoven, and G. Schön (Kluwer Academic, Dordrecht, 1997); S.M. Reimann and M. Manninen, *Rev. Mod. Phys.* **74**, 1283 (2002).
- <sup>2</sup>S.A. Wolf, D.D. Awschalom, R.A. Buhrman, J.M. Daughton, S. von Molnár, M.L. Roukes, A.Y. Chtchelkanova, and D.M. Treger, *Science* **294**, 1488 (2001).
- <sup>3</sup>M. Ciorga, A. Wensauer, M. Pioro-Ladriere, M. Korkusinski, J. Kyriakidis, A.S. Sachrajda, and P. Hawrylak, *Phys. Rev. Lett.* **88**, 256804 (2002).
- <sup>4</sup>J.H. Smet, R.A. Deutschmann, F. Ertl, W. Wegscheider, G. Abstreiter, and K. von Klitzing, *Nature (London)* **415**, 281 (2002).
- <sup>5</sup>S. Tarucha, D.G. Austing, T. Honda, R.J. van der Hage, and L.P. Kouwenhoven, *Phys. Rev. Lett.* **77**, 3613 (1996).
- <sup>6</sup>N. Zabala, M.J. Puska, and R.M. Nieminen, *Phys. Rev. Lett.* **80**, 3336 (1998); *Phys. Rev. B* **59**, 12 652 (1999).
- <sup>7</sup>T. Fujisawa, D.G. Austing, Y. Tokura, Y. Hirayama, and S. Tarucha, *Nature (London)* **419**, 278 (2002).
- <sup>8</sup>H.U. Baranger, D. Ullmo, and L.I. Glazman, *Phys. Rev. B* **61**, R2425 (2000).
- <sup>9</sup>C.-K. Wang and K.-F. Berggren, *Phys. Rev. B* **57**, 4552 (1998).
- <sup>10</sup>H. Jiang, H.U. Baranger, and W. Yang, *Phys. Rev. Lett.* **90**, 026806 (2003).
- <sup>11</sup>E.P.A. Bakkers, Z. Hens, A. Zunger, A. Franceschetti, L.P. Kouwenhoven, L. Gurevich, and D. Vanmaekelbergh, *Nano Lett.* **1**, 551 (2001).
- <sup>12</sup>D. Davidović and M. Tinkham, *Phys. Rev. B* **61**, R16 359 (2000).
- <sup>13</sup>Ph. Jacquod and A.D. Stone, *Phys. Rev. Lett.* **84**, 3938 (2000).
- <sup>14</sup>For instance, for the dot referred to in Fig. 1, the direct bare

Coulomb matrix elements average to  $\langle U_d \rangle = 0.114 \text{ Ry}$ , with a low standard deviation  $\sigma_d = 0.009 \text{ Ry}$ . Among the next leading terms, in contrast, the exchange matrix elements average to  $\langle U_{ex} \rangle = 0.005 \text{ Ry}$  ( $\sigma_{ex} = 0.006 \text{ Ry}$ ).

- <sup>15</sup>It is readily shown that  $\hat{S}^2 = \hat{S}_z(\hat{S}_z + 1) + \hat{N}_\downarrow - \sum_{\nu\nu'}^{\text{occ}} |\langle \varphi_{\nu\uparrow} | \varphi_{\nu'\downarrow} \rangle|^2$ , corresponding to minority spin; see, e. g., A. Szabo and N.S. Ostlund, *Modern Quantum Chemistry: Introduction to Advanced Electronic Structure Theory* (McGraw-Hill, New York, 1989). The last two terms cancel if the orbital basis is orthonormal.
- <sup>16</sup>R. Saniz, B. Barbiellini, and A. Denison, *Phys. Rev. B* **65**, 245310 (2002).
- <sup>17</sup>N. Del Fatti, C. Voisin, M. Achermann, S. Tzortzakis, D. Christofilos, and F. Vallée, *Phys. Rev. B* **61**, 16 956 (2000); I. Nagy, M. Alducin, J.I. Juaristi, and P.M. Echenique, *Phys. Rev. B* **64**, 075101 (2001).
- <sup>18</sup>Note deviations from first Hund’s rule filling in 2D QDs have long been reported. See, e.g., Ref. 5.
- <sup>19</sup>One has  $\Delta p > 0$  also in bulk semiconductors and metals along directions in the Brillouin zone where the spectrum contains a band gap (e.g., along [111] in Cu). In these cases the cutoff momentum is related to the dimension of the Jones or Brillouin zones, respectively. See M.H. Weber *et al.*, *Phys. Rev. B* **66**, 041305(R) (2002).
- <sup>20</sup>The asphericity of the EMD when there are incomplete shells is found to be very small.
- <sup>21</sup>Strictly, of course, there are two separate Fermi momenta associated with the up and down spins in the underlying momentum density distribution explaining the reason for the broadening of  $\Delta p$ .
- <sup>22</sup>We do not contradict the theorem of Lieb and Mattis [*Phys. Rev.*

- 125**, 164 (1962)] regarding the absence of a magnetic ground state in the 1D case because our interaction in Eq. (1) is spin dependent.
- <sup>23</sup>In our model, to observe oscillations in  $\zeta$  it will suffice to have singularities in the noninteracting density of states and a strong  $U$ . Thus it applies to a large class of systems, including the so-called chaotic QDs. For a study of the relation between symmetry and spin polarization see, e.g., I.I. Yakimenko *et al.*, Phys. Rev. B **63**, 165309 (2001). For a discussion of singularities in the density of states of chaotic QDs see, e.g., Matthias Brack and Rajat K. Bhaduri, *Semiclassical Physics* (Addison-Wesley, Reading, 1997).
- <sup>24</sup>A nanowire can be viewed as a very elongated ellipsoid.
- <sup>25</sup>Our  $UN$  is close to the Stoner parameter  $I$  of Ref. 6, both in meaning and in value.
- <sup>26</sup>Off-diagonal terms are generally expected to reduce the ground state polarization. We have independently verified the oscillations of polarization with size in dots containing up to 8 electrons by performing variational quantum Monte Carlo calculations. The variational many-body wave function consisted of Slater determinants built from the noninteracting orbitals with a two-body Jastrow factor to incorporate correlation effects. The Jastrow factor was optimized via the SGA method, see A. Harju *et al.*, Phys. Rev. Lett. **79**, 1173 (1997).